

Neuronal Signaling Optimization for Intrabody Nanonetworks

Junichi Suzuki

Department of Computer Science
University of Massachusetts, Boston
Boston, MA 02125, USA
jxs@cs.umb.edu

Pruet Boonma

Department of Computer Engineering
Chiang Mai University
Chiang Mai, 50200, Thailand
pruet@eng.cmu.ac.th

Dung H. Phan

Department of Computer Science
University of Massachusetts, Boston
Boston, MA 02125, USA
phdung@cs.umb.edu

Abstract—This paper considers natural neurons as a physical communication medium and defines a Time Division Multiple Access (TDMA) communication protocol on top of the physical layer to construct intrabody nanonetworks, each of which networks nanoscale nodes to perform sensing and actuation tasks in the body for biomedical and prosthetic purposes. The proposed protocol, called Neuronal TDMA, leverages a novel evolutionary multiobjective optimization algorithm (EMOA) to seek the optimal signaling schedule for individual nodes in the network with respect to conflicting optimization objectives such as signaling delay and fairness while avoiding signal interference. Simulation results show that the proposed EMOA efficiently obtains quality TDMA signaling schedules and outperforms existing EMOAs.

I. INTRODUCTION

A nanoscale system consists of nanomachines, which are nanoscale devices that perform simple computation, sensing and/or actuation tasks [1], [2]. They may be man-made devices built in the *top-down* approach, downscaling the current microelectronic and micro-electromechanical technologies, or in the *bottom-up* approach, assembling synthesized nanomaterials such as graphene nanoribbons and carbon nanotubes. Alternatively, nanomachines may be *bio-hybrid*, integrating man-made nanostructures with biological materials such as DNA strands and genetically engineered cells, or *bio-enabled*, synthesizing biological materials without man-made nanostructures.

An emerging design strategy for nanoscale systems is to *network* nanomachines for operating in larger physical spaces in higher spatial and temporal resolutions. Although individual nanomachines are limited in computation, sensing and actuation capabilities, an assembly of nanomachines can potentially organize into a “large-scale” network that spreads on centimeter to meter scale and collaboratively performs tasks that no individual nanomachines could.

This paper considers natural neurons as a physical communication medium and defines a Time Division Multiple Access (TDMA) communication protocol, called Neuronal TDMA, on top of the physical layer (Fig. 1) in order to construct intrabody nanonetworks where nanomachines are networked to perform sensing and actuation tasks in the human body for biomedical and prosthetic purposes (e.g., in-situ physiological sensing, biomedical anomaly detection, neural signal transduction and neuroprosthesis control). A neuron-based intrabody nanonetwork consists of a set of nanoscale sensor/actuator nodes and a network of neurons that are artificially formed into a particular topology. It allows individual nodes to interface with neurons

and communicate to other nodes with neuronal (i.e., electrochemical) signals through a chain of neurons. Neuron-based communication possesses advantages such as biocompatibility, energy efficiency, long distance coverage, high speed signaling (up to 90 m/s) and low signal attenuation over other intrabody communication schemes (e.g., electromagnetic schemes) [3].

Neuronal TDMA performs single-bit TDMA scheduling for individual nodes to fire their nearby neurons and multiplex/parallelize signal transmissions in a given neuronal network. It uses a novel evolutionary multiobjective optimization algorithm (EMOA) to seek the Pareto-optimal signaling schedule for nodes in the network with respect to conflicting optimization objectives such as signaling delay and fairness.

The proposed EMOA, called SMSP-EMOA, heuristically seeks the optimal TDMA schedules (i.e., which neurons to fire and when to fire them to trigger signal transmissions) for nodes by evolving a set of solution candidates (or *individuals*) via various operators (e.g., crossover and selection operators) through generations. Each individual represents a particular TDMA schedule for nodes with respect to time. SMSP-EMOA addresses an important issue in neuronal signaling: *interference*. When different signals attempt to travel through a neuron simultaneously, they interfere (or collide) with each other. This leads to the loss or corruption of information encoded with the signals. SMSP-EMOA is designed to avoid signal interference to ensure that signals reach the destination while multiplexing/parallelizing signal transmissions.

SMSP-EMOA is designed as an *indicator-based* EMOA, which leverages a *quality indicator* in its selection operators [4]. A quality indicator measures the goodness of each individual. For example, the hypervolume indicator [5], or the S metric, and its variants have been used in various EMOAs. Recent research findings (e.g., [6]) show that indicator-based EMOAs outperform traditional EMOAs. SMS-EMOA (S Metric Selection EMOA) is one of the most successfully and widely used indicator-based EMOAs [7]. It uses the hypervolume indicator in its environmental selection operator, which chooses a set of individuals used in the next generation from the union of the current population and its offspring.

SMSP-EMOA extends SMS-EMOA with a quality indicator, called *prospect indicator*. The prospect indicator measures the potential (or prospect) of each individual to reproduce offspring that dominate itself and spread out in the objective space. SMSP-EMOA uses the prospect indicator in its parent

selection operator, which chooses parent individuals from the population to reproduce offspring, as well as the hypervolume indicator in its environmental selection operator. The prospect indicator allows the parent selection operator to (1) maintain sufficient selection pressure to improve convergence velocity toward the Pareto-optimal front, and (2) diversify individuals to spread out individuals in the objective space.

Simulation results show that SMSP-EMOA efficiently obtains quality TDMA schedules with acceptable computational costs and allows nanomachines to perform neuronal signal transmissions while avoiding signal interference. It outperforms several well-known existing EMOAs.

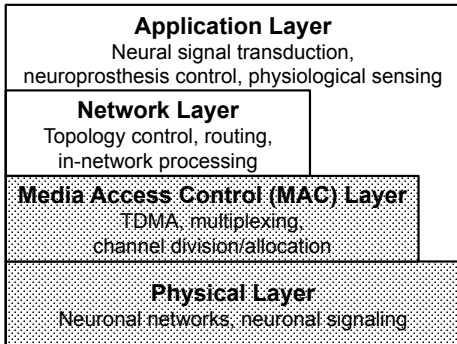


Fig. 1. Neuronal TDMA positioned at the MAC layer in the Traditional Layered Architecture for Computer Communications. This paper focuses on the physical and MAC layers for neuronal signaling.

II. BACKGROUND

This section provides some background on neuronal signaling and neuron-based intrabody nanonetworks.

A. Neuronal Signaling

Neurons are a fundamental component of the nervous system, which includes the brain and the spinal cord. They are electrically excitable cells that process and transmit information via electrical and chemical signaling. A neuron consists of cell body (or soma), dendrites and axon (Fig. 2). A soma varies from 4 to 100 micrometers in diameter. Dendrites are thin structures that arise from the soma. The length of a dendrite is up to a few hundred micrometers. Dendrites receive the majority of inputs to a neuron. An axon is a cellular extension that arises from the soma. It travels through the body in bundles called *nerves*. Its length can be over one meter in the human nerve that arises from the spinal cord to a toe.

Neurons are connected with each other to form a network. They communicate via *synapses*, each of which is a junction between two neurons. A synapse contains molecular machinery that allows a (presynaptic) neuron to transmit a chemical signal to another (postsynaptic) neuron. Signals are transmitted from the axon of a presynaptic neuron to a dendrite of a postsynaptic neuron. An axon transmits an output signal to a postsynaptic neuron, and a dendrite receives an input signal from a presynaptic neuron.

Presynaptic and postsynaptic neurons maintain voltage gradients across their membranes by means of voltage-gated ion channels, which are embedded in the presynaptic membrane to unbalance intracellular and extracellular concentration of ions (e.g., Ca^{2+}). Changes in the cross-membrane ion concentration (i.e., voltage) can alter the function of ion channels.

If the concentration changes by a large enough amount (e.g., approx. 80 mV in a giant squid), ion channels start pumping extracellular ions inward. Upon the increase in intracellular ion concentration, the presynaptic neuron releases a chemical called a *neurotransmitter* (e.g., acetylcholine), which travels through the synapse from the presynaptic postsynaptic neuron. The neurotransmitter electrically excites the postsynaptic neuron, which in turn generates an electrical pulse called an *action potential*. This signal travels rapidly along the neuron's axon and fires synaptic connections (i.e., opens ion channels) when it arrives at the axon's terminals. This way, an action potential triggers cascading neuron-to-neuron communication.

Fig. 3 shows how Ca^{2+} concentration changes in a neuron. When the concentration peaks, the neuron releases a neurotransmitter(s) and goes into a *refractory period* (T_r in Fig. 3), which is the time required for the neuron to replenish its internal Ca^{2+} store. During T_r , it cannot process any incoming signals. The refractory period is approximately two milliseconds in a giant squid.

B. Neuron-based Intrabody Nanonetworks

This paper assumes neuronal signaling in a network of neurons that are artificially grown and formed into particular topology patterns. This assumption is made upon numerous research efforts to grow neurons on substrates and form topologically-specific neuronal networks (e.g., [8]).

Fig. 4 illustrates a schematic neuron-based intrabody nanonetwork. It contains an artificially-grown neuronal network and several nanomachines such as sensors and a sink. Sensors utilize neuronal signaling to deliver sensor data to a sink. As a potential application, sensors may periodically monitor certain physiological status and report physiological data or biomedical anomalies to the sink. The sink may work as a transducer that converts incoming electrochemical signals to electrostatic or electromagnetic signals. Electrostatic signals may carry sensor data to an on-body (i.e., epidermal) device(s) through a body-coupled communication scheme [9]. Electromagnetic signals may carry sensor data to an around-body device(s) such as a smartphone and tablet computer.

Other potential applications are neurointerfaces that utilize in-situ sensing and actuation for prostheses; for example, neuroprosthetic bladder control (Fig. 5). In a normal bladder, a sensory nerve senses that the bladder is full of urine and transmits a sensory signal (i.e., the bladder's sense of fullness) to the brain. Whenever appropriate, the brain sends a control signal through the spinal cord to contract the bladder, relax the sphincter and trigger urination. However, nervous system disorders (e.g., spinal cord injuries and subsequent paralysis) can disrupt those signals to/from the brain and eliminate the fullness sensation and muscle control. Patients with these disorders are forced to empty their bladders with catheters.

In-situ sensing and actuation can help correct incontinence. In Fig. 5, a particular portion of a spinal nerve, called dorsal root ganglion, is teased out and interfaced to sensor nodes. The sensors intercept neuronal signals from the nerve and forwards them to the sink node. The sink may determine whether the bladder is full, and if it is full, transmits electrostatic or electromagnetic signals to an on/around-body node(s), which in turn notifies the bladder's fullness to the patient. A neurostimulator(s) connected to the nerve issues high-frequency

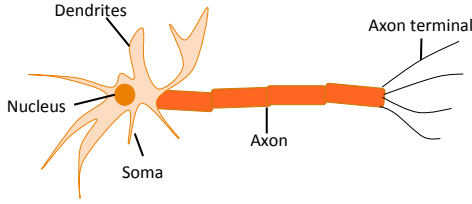


Fig. 2. The structure of neurons

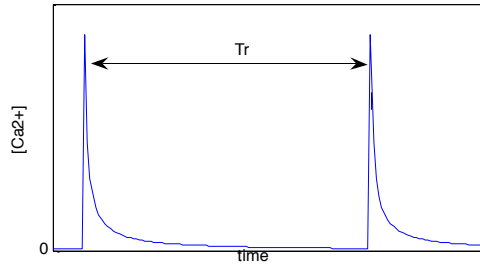


Fig. 3. Intracellular Ca^{2+} concentration

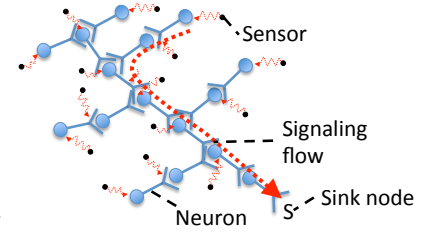


Fig. 4. An Example Sensor-Actuator Network

stimulation to prevent the bladder from emptying itself. Whenever ready to urinate, the patient uses his/her on/around-body node to issue an electrostatic or electromagnetic signal to a subepidermal node, which transduces it to a neuronal electrochemical signal and transmits it to in-situ a neurostimulator(s). Each neurostimulator delivers low-frequency stimulation or stop stimulation so that the bladder to empty. This intervention can be a less invasive alternative to the current state of the art in neuroprosthetic bladder control (e.g., [10]).

This paper assumes that nanomachines (e.g., sensors) interact with neuronal networks in a *non-invasive* manner. This means that it is not required to insert particular materials (e.g., carbon nanotubes) into neurons so that nanomachines can trigger and receive signals. For example, nanomachines may use chemical agents (e.g., acetylcholine and mecamylamine [11]) or light [12].

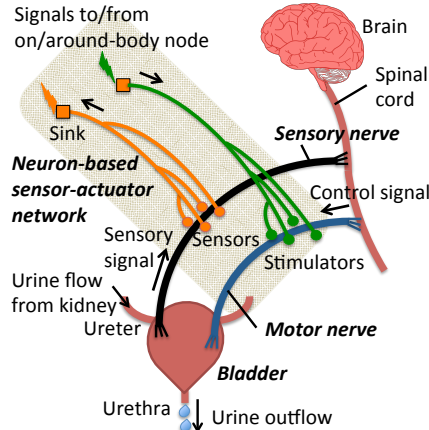


Fig. 5. Neuroprosthetic Bladder Control

III. NEURONAL TDMA

Neuronal TDMA performs a single-bit TDMA communication that periodically assigns a *time slot* to each sensor. Sensors fire neurons, one after the other, each using its own time slot. This allows multiple sensors to transmit signals to the sink through the shared neuronal network. Each sensor transmits a single-bit within a single time slot. This single-bit-per-slot design is based on two assumptions: (1) a signal (i.e., action potential) is interpreted with two levels of amplitudes, which represent 0 and 1, and (2) after a signal transmission, a neuron goes into a refractory period (T_r in Fig. 3).

As described in Section I, an important goal of Neuronal TDMA is to avoid signal interference, which occurs when multiple signals fire the same neuron at the same time and leads to corruption of transmitted sensor data at the sink.

Signals can easily interfere with each other if sensors fire their neighboring neurons randomly. Neuronal TDMA is intended to eliminate signal interference by scheduling which sensors fire which neurons with respect to time. The proposed EMOA seeks the optimal TDMA schedules for a set of sensors in a given neuronal network.

Fig. 6 shows an example neuronal network that has five neurons (n_1 to n_5) and four nodes (three sensors, s_1 , s_2 and s_3 , and a sink). Fig. 7 illustrates an example TDMA schedule for those sensors to fire neurons. The scheduling cycle period lasts five time slots ($T_s = 5$). The sensor s_1 fires the neuron n_4 to initiate signaling in the first time slot T_1 . The signal travels through n_5 in the next time slot T_2 to reach the sink. s_2 transmits a signal on n_3 in T_2 . During T_2 , two signals travel in the neuronal network in parallel. The duration of each time slot (T_u in Fig. 7) is designed as the sum of three time periods: (1) *synaptic delay*, which is the time for neurotransmitters to travel through a synapse from a presynaptic neuron or a sensor and generate an action potential in a postsynaptic neuron, (2) *intracellular transmission delay*, which is the time for an action potential to travel within a neuron (i.e., from its dendrite terminal to its axon terminal) and (3) a refractory period.

Neuronal TDMA considers three optimization objectives: (1) signaling yield, (2) signaling fairness among sensors and (3) signaling delay. Signaling yield (f_Y) is computed as follows. It is to be maximized.

$$f_Y = \sum_{i=1}^M |E^{s_i}| \quad (1)$$

This objective indicates the total number of signals that the sink receives from all M sensors during T_s .

Signaling fairness (f_F), is computed as follows. It is to be maximized.

$$f_F = \sum_{l=1}^M \sum_{m=1}^M \sum_{k=1}^{|E^{s_l}|} \frac{1}{|t_d^{k(s_l)} - t_d^{k(s_m)}|}, \quad l \neq m \quad (2)$$

$t_d^{k(s_l)}$ denotes the departure time of the k -th signal that s_l transmits to the sink. This objective encourages sensors to equally access the shared neuronal network for signaling in order to avoid a situation where a limited number of sensors dominate the network. Higher fairness means that sensors access the neuronal network more equally.

Signaling delay (f_D), is computed as follows. It is to be minimized.

$$f_D = \max_{s_i \in S} t_a^{|E^{s_i}|}((s_i)) \quad (3)$$

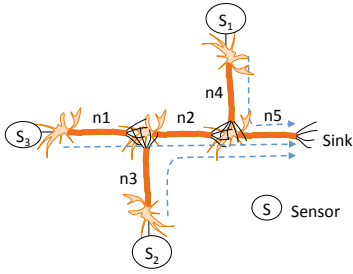


Fig. 6. An Example Neuronal Network

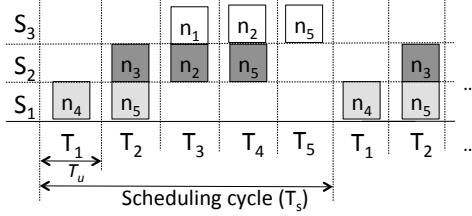


Fig. 7. An Example TDMA Schedule

	T_1	T_2	T_3	T_4	T_5
S_3	0	0	1	0	0
S_2	0	1	0	0	0
S_1	1	0	0	0	0

Fig. 8. An Example Individual

$t_a^{|E^{s_i}|}((s_i))$ denotes the arrival time at which the sink receives the last (the $|E^{s_i}|$ -th) signal that s_i transmits. f_D indicates how soon the sink receives all signals from all M sensors. f_D determines the scheduling cycle period T_s ($T_s = f_D$).

Neuronal TDMA considers three constraints in its optimization process. The first constraint enforces that at most one signal can pass through each neuron in a single time slot. The second constraint enforces each sensor transmit at least one signal to the sinks ($|E^{s_i}| \geq 1 \forall i = 1, 2, \dots, M$). The third constraint (C_D) is the upper limit for f_D : $f_D \leq C_D$. The delay constraint violation (g_D) is computed as follows where $I = 1$ if $f_D > C_D$ and $I = 0$ otherwise.

$$g_D = I \times (f_D - C_D) \quad (4)$$

IV. THE PROPOSED EMOA: SMSP-EMOA

A. Individual Representation

Each individual represents a particular TDMA schedule for M sensors. Fig. 8 shows the structure of an example individual that represents a TDMA schedule described in Fig. 7. In this example, the first sensor, s_1 , fires the first neuron n_1 for signaling. The signal travels through two neurons, n_2 and n_3 , in the second and third time slots t_2 and t_3 , respectively.

B. Algorithmic Structure

Algorithm 1 shows SMSP-EMOA's algorithmic structure.

Algorithm 1 The Algorithmic Structure of SMSP-EMOA

```

1:  $t = 0$ 
2:  $\mathcal{P}_0 = \text{initializePopulation}(\mu)$ 
3: while  $t < T_{max}$  do
4:    $p_1 = \text{prospectBasedParentSelection}(\mathcal{P}_t)$ 
5:    $p_2 = \text{prospectBasedParentSelection}(\mathcal{P}_t)$ 
6:   if  $\text{random}() \leq P_c$  then
7:      $o = \text{crossover}(p_1, p_2)$ 
8:   end if
9:   if  $\text{random}() \leq P_m$  then
10:     $o = \text{mutation}(o)$ 
11:   end if
12:    $\mathcal{P}_t = \mathcal{P}_t \cup o$ 
13:    $\mathcal{P}_{t+1} = \text{hypervolumeBasedEnvSelection}(\mathcal{P}_t)$ 
14:    $t = t + 1$ 
15: end while

```

In the first iteration ($t = 0$), μ individuals are randomly generated as the initial population \mathcal{P}_0 (Line 2). In each iteration (t), a pair of individuals, called parents (p_1 and p_2), are chosen from the current population \mathcal{P}_t with the proposed parent selection operator, which uses the prospect indicator ($\text{prospectBasedParentSelection}()$, Lines 4 and 5).

With the crossover rate P_c , two parents reproduce one offspring with the SBX (self-adaptive simulated binary crossover) operator [13] (Lines 6 and 7). Polynomial mutation [14] is performed on the offspring with the mutation rate of P_m (Lines 9 to 10). The offspring is combined with the population \mathcal{P}_t to form a pool of candidate individuals used in the next iteration ($t = t + 1$).

Environmental selection follows reproduction. One individual is eliminated from \mathcal{P}_t to produce \mathcal{P}_{t+1} ($\text{hypervolumeBasedEnvSelection}()$, Line 13). Environmental selection performs a $(\mu + 1)$ steady state evolution.

C. Parent Selection with the Prospect Indicator

Algorithm 2 shows how the proposed parent selection operator ($\text{prospectBasedParentSelection}()$ in Algorithm 1) works with the prospect indicator. It is designed as a variant of binary tournament selection. It randomly draws two individuals from the current population \mathcal{P} , compares them based on the *dominance* relationship between them and chooses a superior one as a parent (Lines 5 to 8). Note that p_1 is said to *dominate* p_2 (denoted by $p_1 \succ p_2$) if the both of the following conditions are satisfied: (f_i denotes the i -th objectives.)

- $f_i(\vec{x}) \leq f_i(\vec{y}) \forall i = 1, \dots, n$
- $f_i(\vec{x}) < f_i(\vec{y}) \exists i = 1, \dots, n$

If two individuals (p_1 and p_2) do not dominate each other and are placed in the same rank, the proposed selection operator chooses one of them as a parent with the prospect indicator. Lines 10 and 11 compute the prospect indicator values of p_1 and p_2 ($I_P(p_1)$ and $I_P(p_2)$), and Line 12 compares the two values. The proposed operator chooses the one with a higher I_P value (Lines 12 to 16).

The prospect indicator value of an individual i ($I_P(i)$) is computed as follows:

$$I_P(i) = V(\mathcal{R}_{rank(i)}) - V(\mathcal{R}_{rank(i)} \setminus \{i\}) \quad (5)$$

$rank(i)$ denotes the value of a rank that i is placed at. $\mathcal{R}_{rank(i)}$ denotes a set of individuals that are placed at the rank of $rank(i)$. \mathcal{R}_1 contains the individuals of the best (or highest) rank (i.e., the non-dominated individuals in \mathcal{P}). \mathcal{R}_2 contains the individuals of the second highest rank (i.e., individuals that are non-dominated in $\mathcal{P}_t \setminus \mathcal{R}_1$). $V(\mathcal{R})$ denotes the volume of a hypercube that dominates the individuals in \mathcal{R} in the objective space. It is calculated with the Lebesgue measure as follows.

$$V(\mathcal{R}) = \Lambda \left(\bigcup_{x \in \mathcal{R}} \{x' | x_u \succ x' \succ x\} \right) \quad (6)$$

x_u denotes the Utopian point, and Λ denotes the Lebesgue measure.

The prospect indicator evaluates the potential (or prospect) of an individual to reproduce offspring that dominate itself. Fig. 9 shows an example measurement of the prospect indicator in a two dimensional objective space. This example considers three non-dominated individuals: a , b and c ($\mathcal{R}_{rank(a)} = \mathcal{R}_{rank(b)} = \mathcal{R}_{rank(c)} = \{a, b, c\}$). The Utopian point is $(0, 0)$. $I_P(b)$ is a shaded area in Fig. 9 (i.e., $V(\mathcal{R}_{rank(b)} - V(\mathcal{R}_{rank(b)} \setminus \{b\}))$).

Algorithm 2 prospectBasedParentSelection()

Require: $\mathcal{P} | \mathcal{P} \neq \emptyset$
1: $p_1 = \text{randomSelection}(\mathcal{P})$
2: $p_2 = \text{randomSelection}(\mathcal{P})$
3: **if** $p_1 = p_2$ **then**
4: **return** p_1
5: **else if** $p_1 \succ p_2$ **then**
6: **return** p_1
7: **else if** $p_2 \succ p_1$ **then**
8: **return** p_2
9: **else**
10: $I_P(p_1) = \text{prospectIndicator}(p_1, \mathcal{R}_{rank(p_1)})$
11: $I_P(p_2) = \text{prospectIndicator}(p_2, \mathcal{R}_{rank(p_2)})$
12: **if** $I_P(p_1) > I_P(p_2)$ **then**
13: **return** p_1
14: **else**
15: **return** p_2
16: **end if**
17: **end if**

Algorithm 3 shows how to compute $I_P(p)$. \mathcal{P} denotes a set of individuals that are placed at the same rank as an individual p . For each objective (o), the distance between p and s is measured to compute $I_P(p)$, where s denotes an individual that yields the closest yet superior objective value.

Algorithm 3 prospectIndicator()

Require: $p, \mathcal{P} | \mathcal{P} \neq \emptyset$
1: $v = 1$
2: **for each** $o \in \mathcal{O}$ **do**
3: $s = \emptyset$
4: **for each** $n \in \mathcal{P}$ **do**
5: **if** $f_o(n) < f_o(p)$ **then**
6: **if** $s = \emptyset$ **then**
7: $s = n$
8: **else if** $f_o(s) < f_o(n)$ **then**
9: $s = n$
10: **end if**
11: **end if**
12: **end for**
13: $v = v \times |f_o(p) - f_o(s)|$
14: **end for**
15: **return** v

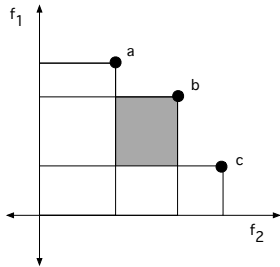


Fig. 9. An Example Measurement of Prospect Indicator

D. Environmental Selection with the Hypervolume Indicator

Algorithm 4 shows how environmental selection (`hypervolumeBasedEnvSelection()` in Algorithm 1)

works with the hypervolume indicator. In environmental selection, μ individuals are selected from $\mu + 1$ individuals as the population used in the next iteration.

`dominanceRanking()` performs dominance ranking on the current population \mathcal{P} (Line 1). \mathcal{R}_1 and \mathcal{R}_v contain the best-ranked and worst-ranked individuals, respectively. In Lines 2 and 3, an individual p is discarded from \mathcal{R}_v . p is an individual that yields the minimum value of *exclusive hypervolume contribution* I_H . I_H of an individual $i \in \mathcal{R}_v$ is computed as follows:

$$I_H(i) = H(\mathcal{R}_v) - H(\mathcal{R}_v \setminus \{i\}) \quad (7)$$

$H(\mathcal{R}_v)$ denotes the volume of a hypercube that the worst-ranked individuals dominate. It is calculated with the Lebesgue measure as follows.

$$H(\mathcal{R}_v) = \Lambda \left(\bigcup_{x \in \mathcal{R}_v} \{x' | x \succ x' \succ x_r\} \right) \quad (8)$$

x_r denotes a reference point in the objective space. Fig. 10 shows an example measurement of I_H in a two dimensional objective space. This example considers three individuals in \mathcal{R}_v : a , b and c . $x_r = (r_1, r_2)$. $I_H(b)$ is a shaded area in Fig. 10 (i.e., $H(\mathcal{R}_v) - H(\mathcal{R}_v \setminus \{b\})$).

Algorithm 4 hypervolumeBasedEnvSelection()

Require: $\mathcal{P} | \mathcal{P} \neq \emptyset$
1: $\{\mathcal{R}_1, \mathcal{R}_2, \dots, \mathcal{R}_v\} = \text{dominanceRanking}(\mathcal{P})$
2: $p = \text{argmin}_{s \in \mathcal{R}_v} [I_H(s)]$
3: $\mathcal{P} = \mathcal{P} \setminus p$
4: **return** \mathcal{P}

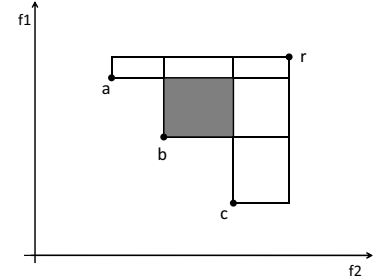


Fig. 10. An Example Measurement of Exclusive Hypervolume Contribution

V. SIMULATION EVALUATION

This section evaluates SMSP-EMOA through simulations. A simulated neuronal network is obtained with a two-step procedure. The first step utilizes NeuGen [15] to generate a network of N neurons. The second step forms a tree structure with those neurons based on a randomized L -ary tree construction algorithm. This algorithm generates a rooted tree in which each neuron has no more than $\mathcal{N}(L, (L + 1)^2)$ child neurons. \mathcal{N} denotes a normal distribution. L and $L + 1$ are the mean and the standard deviation of the number of child neurons for each neuron. This paper uses a randomized 2-ary (i.e., binary) tree that contains 40 neurons and 10 sensors.

SMSP-EMOA is configured with a set of parameters shown in Table I. Q denotes the total number of time slots in an individual ($Q = 15$ in Fig. 8). Every simulation result is the average of the results from 20 independent simulations. SMSP-EMOA is compared with two existing EMOAs: NSGA-II [14] and SMS-EMOA [7]. They are configured with Table I. All other configurations follow those described in [14] and [7].

Fig. 11 shows how SMSP-EMOA, SMS-EMOA and NSGA-II individuals increase the union of the hypervolumes

that they dominate in the objective space as the number of generations grows. The hypervolume metric quantifies the optimality and diversity of individuals [5]. A higher hypervolume means that individuals are closer to the Pareto-optimal front and more diverse in the objective space. As Fig. 11 shows, all three EMOAs rapidly increase their hypervolume measures in the first 10 generations. NSGA-II converges around the 45th generation. SMSP-EMOA and SMS-EMOA converge around the 60th generation. Fig. 11 demonstrates that SMSP-EMOA efficiently evolve individuals and improve their quality and diversity within 100 generation.

Table II shows the average of each objective value at the last generation. A value in parentheses indicates a standard deviation of objective values. Fig. 11 and Table II demonstrate that SMSP-EMOA performs TDMA scheduling optimization efficiently and effectively for neuronal signaling.

TABLE I. PARAMETER CONFIGURATIONS

Parameter	Value
Max. # of generations in each simulation	100
Population size	100
Crossover rate	0.9
Mutation rate	1/Q

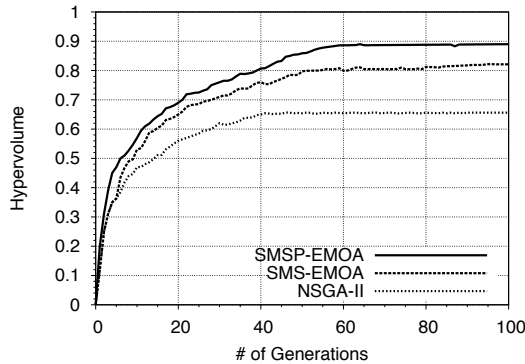


Fig. 11. Hypervolume Measurement

TABLE II. OBJECTIVE FUNCTION VALUES

	Yield (f_Y)	Fairness (f_F)	Delay (f_D)
SMSP-EMOA	22.12 (3.98)	0.14 (0.4)	21.09 (3.11)
SMS-EMOA	20.17 (4.12)	0.12 (0.4)	23.17 (3.11)
NSGA-II	16.11 (3.22)	0.08 (0.10)	29.78 (6.91)

VI. RELATED WORK

Balasubramaniam et al. first examined TDMA-based neuronal signaling [11]. This paper extends it with an indicator-based EMOA that considers conflicting optimization objectives such as signaling yield and delay.

SMSP-EMOA extends SMS-EMOA's parent selection operator with the prospect indicator. While SMS-EMOA uses the hypervolume indicator for its environmental selection, it uses no indicators for its parent selection. Instead, it randomly draws two parent individuals from the population [7]. SMSP-EMOA performs a binary tournament with the prospect indicator for parent selection.

SPAM is similar to SMSP-EMOA in that it uses multiple indicators as SMSP-EMOA does [16]. It can use two or more indicators in its environmental selection operator. Unlike SPAM, SMSP-EMOA uses different indicators (the prospect and hypervolume indicators) in different (parent and environmental) selection operators.

SMSP-EMOA is studied in [17] with well-known test problems such as ZDT and DTLZ problem families. This paper examines it in a more realistic problem, neuronal signaling optimization in intrabody nanonetworks, with problem-specific objectives, constraints and individual representation. Simulation results show that SMSP-EMOA can effectively solve the problem beyond test problems.

VII. CONCLUSION

This paper formulates an optimization problem for neuronal signaling and solves the problem with an EMOA, called SMSP-EMOA. Simulation results show that SMSP-EMOA efficiently obtains quality TDMA schedules with acceptable computational costs and allows nanomachines to perform neuronal signal transmissions while avoiding signal interference. It outperforms several well-known existing EMOAs.

REFERENCES

- [1] T. Suda, M. Moore, T. Nakano, R. Egashira, and A. Enomoto, "Exploratory research on molecular communication between nanomachines," in *Proc. ACM Genetic and Evol. Computat. Conference*, 2005.
- [2] T. Nakano, A. Eckford, and T. Haraguchi, *Molecular Communication*. Cambridge University Press, 2013.
- [3] L. P. Gine and I. F. Akyildiz, "Molecular communication options for long range nanonetworks," *Computer Networks*, vol. 53, 2009.
- [4] C. C. Coello, "Evolutionary multi-objective optimization: Some current research trends and topics that remain to be explored," *Front. Computat. Sci. China*, vol. 3, no. 1, 2009.
- [5] E. Zitzler and L. Thiele, "Multiobjective optimization using evolutionary algorithms: A comparative study," in *Proc. Int'l Conf. on Parallel Problem Solving from Nature*, 1998.
- [6] T. Wagner, N. Beume, and B. Naujoks, "Pareto-, aggregation-, and indicator-based methods in many-objective optimization," in *Proc. Int'l Conf. Evol. Multi-criterion Optimization*, 2007.
- [7] N. Beume, B. Naujoks, and M. Emmerich, "SMS-EMOA: Multiobjective selection based on dominated hypervolume," *European Journal of Operational Research*, vol. 181, no. 3, pp. 1653–1669, 2007.
- [8] S. Pautot, C. Wyart, and E. Y. Isacoff, "Colloid-guided assembly of oriented 3D neuronal networks," *Nat. Methods*, vol. 5, no. 8, 2008.
- [9] T. Zimmerman, "Personal area networks (PAN): Near-field intra-body communication," *IBM Systems Journal*, vol. 35, no. 3-4, 1996.
- [10] D. J. Chew, L. Zhu, E. Delivopoulos, I. R. Mineev, K. M. Musick, C. A. Mosse, M. Craggs, N. Donaldson, S. P. Lacour, S. B. McMahon, and J. W. Fawcett, "A microchannel neuroprosthesis for bladder control after spinal cord injury in rat," *Sci. Transl. Med.*, vol. 5, no. 210, 2013.
- [11] S. Balasubramaniam, N. T. Boyle, A. Della-Chiesa, F. Walsh, A. Mardinoglu, D. Botvich, and A. Prina-Mello, "Development of artificial neuronal networks for molecular communication," *Nano Communication Networks*, vol. 2, no. 2-3, 2011.
- [12] C. Hosokawa, Y. Sakamoto, S. N. Kudoh, Y. Hosokawa, and T. Taguchi, "Femtosecond laser-induced stimulation of a single neuron in a neuronal network," *Appl. Phys. A*, vol. 110, no. 3, 2013.
- [13] K. Deb, K. Sindhya, and T. Okabe, "Self-adaptive simulated binary crossover for real-parameter optimization," in *Proc. of ACM Genetic and Evol. Computat. Conference*, 2007.
- [14] K. Deb, A. Pratap, S. Agarwal, and T. Meyarivan, "A fast and elitist multiobjective genetic algorithm: NSGA-II," *IEEE Trans Evol. Computat.*, vol. 6, no. 2, 2002.
- [15] J. P. Eberhard, A. Wanner, and G. Wittum, "NeuGen: A tool for the generation of realistic morphology of cortical neurons and neural networks in 3D," *Neurocomputing*, vol. 70, no. 1-3, pp. 327–342, 2006.
- [16] E. Zitzler, L. Thiele, and J. Bader, "SPAM: Set preference algorithm for multiobjective optimization," in *Proc. of Int'l Conference on Parallel Problem Solving From Nature*, 2008.
- [17] D. H. Phan, J. Suzuki, and P. Boonma, "SMSP-EMOA: Augmenting sms-emoa with the prospect indicator for multiobjective optimization," in *Proc. IEEE Int'l Conf. on Tools with Artificial Intelligence*, 2011.